ARTICLE

Assessment of shear strength from measuring while drilling shafts in Florida limestone

Michael Rodgers, Michael McVay, David Horhota, Jon Sinnreich, and Jose Hernando

Abstract: The focus of this research is the real-time assessment of drilled shaft capacity based on the unconfined compressive strength (q_u) obtained from measuring while drilling (MWD). Measures of q_u, a function of rock strength commonly used in drilled shaft design, are provided through five monitored drilling parameters: torque, crowd, rotational speed, penetration rate, and bit diameter. Monitored shaft installations took place at three separate locations on drilled shafts, which were subsequently load tested. Using the q_u values obtained from MWD, side shear was estimated in portions of each shaft where instrumented segments indicated the side shear was fully mobilized for direct comparison. To consider all of the current side shear equations used in Florida drilled shaft design, the estimation of tensile strength (q_t) in real time was also needed. This led to a theoretical approach to establish the q_t/q_u relationship that was later verified empirically and provided new correlations between material and mechanical properties of Florida geomaterials. A comparative analysis indicated that the results from multiple established side shear equations, used with q_u from MWD, align well with the results obtained from load testing. This suggests that estimating drilled shaft capacity from MWD is viable to reduce spatial uncertainty.

Key words: drilled shaft, rock auger, measuring while drilling, Florida limestone, specific energy.

Résumé : L'objectif de cette étude est l'évaluation en temps réel de la capacité du puits foré basé sur la résistance en compression simple (q_u) obtenue à partir de la mesure en cours de forage (MWD). Les mesures de q_u, une fonction de la résistance de la roche communément utilisée dans la conception des puits forés, sont fournies par cinq paramètres de forage surveillés : couple, foule, vitesse de rotation, vitesse de pénétration et diamètre du trépan. Des installations à puits contrôlé ont eu lieu à trois endroits différents sur des puits forés qui ont ensuite été soumis à des essais de charge. En utilisant les valeurs de q_u obtenues à partir de MWD, le cisaillement latéral a été estimé dans des parties de chaque puits où des segments instrumentés ont indiqué que le cisaillement latéral était entièrement mobilisé pour une comparaison directe. Afin de prendre en compte toutes les équations de cisaillement latéral utilisées dans la conception des puits forés en Floride, l'estimation de la résistance à la traction (q_t) en temps réel était également nécessaire. Cela a conduit à une approche théorique pour établir la relation q_t/q_u qui a ensuite été vérifiée empiriquement et a fourni de nouvelles corrélations entre les propriétés matérielles et mécaniques des géomatériaux de la Floride. Une analyse comparative a indiqué que les résultats de plusieurs équations de cisaillement latéral établies, utilisées avec q_u de MWD, s'harmonisent bien avec les résultats obtenus à partir des essais de charge. Ceci suggère que l'estimation de la capacité de puits foré par MWD est viable pour réduire l'incertitude spatiale. [Traduit par la Rédaction]

Mots-clés : puits foré, tarière à roche, mesure en cours de forage, calcaire de Floride, énergie spécifique.

Introduction

This paper explores using measurements of unconfined compressive strength, obtained from measuring while drilling shafts, to estimate side shear capacity in real time. The research discussed is part of a larger project that included a laboratory and field drilling investigation using rock augers. From the laboratory investigation, a unique relationship was developed between specific energy (Teale 1965) and unconfined compressive strength, q_u, for Florida limestone (Rodgers et al. 2018a). Specific energy, e, is provided in real time by continuously measuring five drilling parameters: torque, crowd, rotational speed, penetration rate, and bit diameter. The e vs. q_u equation developed from the unique relationship was used during field drilling to assess q_u in real time at the following three separate locations where each monitored drilled shaft was subsequently load tested (Rodgers et al. 2018b):

1. The Little River Bridge site in Quincy, Fla.
2. Florida Department of Transportation (FDOT)'s Kanapaha site in Gainesville, Fla.
3. The Overland Bridge site in Jacksonville, Fla.

The focus of the field investigation was to evaluate the monitored drilling process and compare the shaft capacity estimates obtained from measuring while drilling (MWD) with conventional methods such as load tests and core data. This portion of the research covers estimating skin friction in real time through MWD and comparing the results obtained from load testing the monitored shafts. This paper also discusses new correlations developed between material properties and mechanical properties of Florida geomaterials, which include limestone, intermediate geomaterial (IGM), and overconsolidated clays.

M. Rodgers, M. McVay, and J. Sinnreich. Engineering School of Sustainable Infrastructure & Environment, Herbert Wertheim College of Engineering, University of Florida, Gainesville, FL 32611, USA.
D. Horhota and J. Hernando. State Materials Office, Florida Department of Transportation, 5007 Northeast 39th Avenue, Gainesville, FL 32609, USA.
Corresponding author: Michael Rodgers (email: michael.rodgers@essie.ufl.edu).

Fig. 1. Drilled shaft load-transfer diagram. [Color online.]
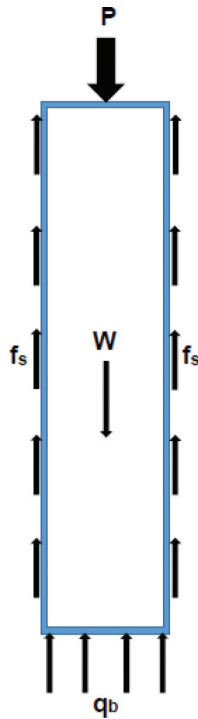
Background

In drilled shaft design, the capacity of each shaft is developed from a combination of end bearing (q_b) and side shear (f_s, commonly referred to as "skin friction"). Axial loads applied to the top of a drilled shaft are transferred to the ground through each resistance mechanism as shown in Fig. 1, where

- P is axial load (kN),
- W is weight of the shaft (kN),
- f_s side shear or skin friction (kPa), and
- q_b is end bearing (kPa).

Load transfer through skin friction is the result of a combination of cohesion and adhesion at the rock–shaft interface. Load transfer through end bearing is the result of compressive loading between the bottom of the drilled shaft and the soil and (or) rock. Although large shaft capacities can be generated through end bearing, due to several factors it is common practice in Florida to design drilled shafts solely using skin friction. These factors include a possible lack of rock layer uniformity beneath each shaft, the possibility of inadequate clean-out at the base of the shaft during excavation leading to a "soft toe" condition, and most importantly the unacceptably large amount of shaft displacement required to fully mobilize end bearing based on load and resistance factor design (LRFD) service limits (AASHTO 2009; Brown et al. 2010; Chung et al. 2012).

In skin friction design, it is common practice to use average layer properties. This allows the engineer to consider multiple rock layers over the span of the shaft, and provides a versatile design approach to account for a high degree of variability. Similar to end bearing, large shaft capacities can also be achieved through rock-socketed side shear. However, the associated shaft displacements are typically less than 1.27 cm (half an inch), which satisfies the LRFD service limits (Brown et al. 2010) and ensures the structure supported by the shaft will experience limited settlement.

When designing drilled shafts, there are numerous methods for estimating skin friction, and typically each equation is only used for a specified material type (e.g., sand, clay or rock). In most cases, equations developed for rock and IGM use unconfined compressive strength, q_u, to estimate side shear capacity (Brown et al. 2010). Therefore, providing real-time measurements of q_u allows the engineer to choose from multiple equations commonly used in design to assess shaft capacity in real time as well. The equations are generally formed using empirical methods and presented in one of the following two ways:

- Using a linear function to develop the equation

$$(1) \qquad f_s = a(q_u)$$

- Or using a power function to develop the equation

$$(2) \qquad f_s = a(q_u)^b$$

where a and b are empirical constants developed using load test data from instrumented drilled shafts. In the pursuit of an accurate method to determine skin friction in real time during field drilling, several of the more common equations used in Florida drilled shaft design were considered for the analysis (Table 1).

Incorporating q_t/q_u ratio into skin friction estimates

As seen in Table 1, all methods use only q_u to estimate skin friction except McVay et al. (1992), hereafter referred to as "McVay et al.", which also incorporates tensile strength, q_t. Using a parametric finite-element method, McVay et al. investigated the maximum side shear at the rock–shaft interface, where they indicated the cohesion of rock is a closely approximated estimate of the failure side shear. However, to determine the cohesion of rock, knowledge of the friction angle is typically needed, which is not readily available. Generally, this requires more than one laboratory strength test to be performed. For example, multiple triaxial compression tests at different confining pressures would be one option, but this is a very time-consuming process. Alternatively, McVay et al. proposed a more simplistic approach using results from unconfined compression and split tension testing implemented on field cores, which are readily available from typical site investigation. They found that the failure of rock can be described through a Mohr–Coulomb strength envelope, leading to the development of an alternative model based on split tension and compressive strength test data.

When compared with conventional test methods, McVay et al. found excellent agreement between results obtained using method 1 (Table 1) with existing q_u and q_t data and the results obtained from 53 pullout tests and seven load tests at 14 different sites in Florida. Furthermore, the method was developed specifically for Florida limestone socketed drilled shafts and recently became the recommended design method in the Florida Department of Transportation (FDOT)'s *Soils and foundation handbook* (SFH; FDOT 2015). As McVay et al. is the SFH recommended design method, measures were taken to ensure the equation could be used for the drilled shaft field-monitoring comparative analysis, which required real-time measurements of tensile strength.

Similar to the e vs. q_u equation developed in Rodgers et al. (2018a), an e vs. q_t equation was also developed. However, the material formation of synthetic limestone used during laboratory drilling was found to provide a higher q_t/q_u ratio than is typical of Florida limestone. This was confirmed in preliminary skin friction analysis at Little River, where McVay et al. used with the laboratory-developed e vs. q_t equation, consistently produced overestimates of side shear. Consequently, alternative methods for determining the q_t/q_u ratio were investigated.

Developing q_t/q_u ratio from boring data

The first method grouped pairs of q_u and q_t values that were collected in the same general vicinity within each approximate

Table 1. Drilled shaft design skin friction equations.

Method	Reference	Design methodology
1	McVay et al. (1992)	$f_s = (1/2)\sqrt{q_u}\sqrt{q_t}$ (kPa)
2	Reese and O'Neill (1987)	$f_s = 0.15q_u$ (kPa)
3	Horvath and Kenney (1979)	$f_s = 6.56\sqrt{q_u}$ (kPa)
4	Williams et al. (1980)	$f_s = 0.3453q_u^{0.367}$ (kPa)
5	Reynolds and Kaderabek (1980)	$f_s = 0.3q_u$ (kPa)
6	Gupton and Logan (1984)	$f_s = 0.2q_u$ (kPa)
7	Carter and Kulhawy (1987)	$f_s = 6.17\sqrt{q_u}$ (kPa)
8	Ramos et al. (1994)	$f_s = 0.5q_u$ (<1724 kPa)
		$f_s = 0.12q_u$ (>1724 kPa)
9	Rowe and Armitage (1987)	$f_s = 14.19\sqrt{q_u}$ (kPa) clean sockets
10	Rowe and Armitage (1987)	$f_s = 18.98\sqrt{q_u}$ (kPa) rough sockets

1.5 m core run, for every boring completed at a site. This was done in an attempt to provide a range of q_t values for each recorded q_u value. Once all the pairs were created, the q_t/q_u ratio was calculated for each pair. Any q_t/q_u value that fell outside of one standard deviation (Std. Dev.) from the mean was removed. Remaining pairs from each boring location were then combined, removing the outliers again, and used to plot q_t vs. q_u to determine the q_t/q_u ratio for the entire site (Fig. 2).

Using the curve-fit q_t/q_u ratio, skin friction was estimated in four segments along the test shaft at the Little River Bridge site where load test results indicated the side shear was mobilized in layers of limestone (Table 2).

As evident in Table 2, using McVay et al. with the developed q_t/q_u ratio provided an excellent result. In all four mobilized sections of the drilled shaft, results obtained from monitoring the shaft installation were in close agreement with the Osterberg load test results. The range of unit side shear values, from all four sections, was indicative of the variability at the site and monitoring was able to distinguish the layers. However, the validity and practicality of the method to determine the site q_t/q_u ratio was in question. Using this approach, the compressive strength values may be paired with split tension values from two dissimilar materials when developing the q_t/q_u ratio. The q_t/q_u ratio developed also does not account for the overestimation of tensile strength that split tension testing provides (Perras and Diederichs 2014). Both cases would provide inaccurate q_t/q_u ratios and shaft capacity estimates in other locations with less available core data. For example, in Table 3 samples 4 and 5 indicate a q_u–q_t pair that would be used to determine the average q_t/q_u ratio for a layer or site to provide q_t for use with the equation. However, upon inspection of the dry unit weights and moisture contents of the two test results, it is clear that these are dissimilar materials that should not be combined and used to determine the q_t/q_u ratio. This led to a more theoretical approach to develop q_t estimations based on Johnston's (1985) criterion.

Development of the Florida geomaterials equation

Johnston (1985), hereafter referred to as "Johnston", investigated the strength of intact geomaterials, where he found that a number of strength criteria can describe the strength of geomaterials and that each criterion is typically limited to certain material types with a limited range of stress conditions. Johnston proposed a new empirical strength criterion that was applicable to a wide variety of intact geomaterials, from lightly overconsolidated (OC) clays to very hard rock, for both compressive and tensile stress regions. His new criterion demonstrated that the strength of these largely different geomaterials followed a distinct progressive pattern.

Based on Johnston's criterion for geomaterials, a q_t/q_u vs. q_u plot was developed by Anoglu et al. (2006) for the concrete industry, indicating that q_t/q_u ratios decrease as compressive strength increases and that the trend is nonlinear. Anoglu et al. tested various concrete samples that were developed using different water-to-cement ratios, binders, additives, cure times, and curing conditions, which is similar to the various limestone formations found throughout Florida. Specifically, each geological formation is a unique matrix comprising different binding material concentrations, different constituents within the rock matrix such as clay found in north Florida that is not found in south Florida, various formation ages ranging from less than 1 million years to over 35 million years, various curing conditions such as changing sea level or the amount of overburden present above the formation, as well as different skeletal remains left behind that act as the aggregate and provide the main source of binder from calcite precipitate.

In Johnston's report, he indicated a similar q_t/q_u vs. q_u relationship could be determined for all geomaterials. Therefore, using Johnston's proposed criterion, an equation similar to Anoglu et al.'s (2006) was developed for Florida geomaterials. The equation development began using Johnston's relationship for q_t/q_u ratios

$$(3) \qquad \frac{q_t}{q_u} = \frac{B}{M}$$

where

- q_t is uniaxial tensile strength (direct tension).
- q_u is uniaxial compressive strength.
- B is a material parameter, independent of material type, developed by Johnston that defines the nonlinearity of the Mohr–Coulomb failure envelope and is a measure of confinement effectiveness.
- M is also a material parameter developed by Johnston, and defines the changes in failure stresses associated with different geomaterial types (i.e., the relationship between effective friction angle, ϕ', and q_u that would be obtained from multiple triaxial tests).

Johnston developed a single equation for B

$$(4) \qquad B = 1 - 0.0172(\log q_u)^2$$

where q_u is measured in kilopascals (kPa), and developed multiple equations for M based on material groupings, such as carbonate materials with well-developed crystal cleavage (e.g., limestone and dolomite),

$$(5) \qquad M = 2.065 + 0.170(\log q_u)^2$$

lithified argillaceous materials (e.g., OC clay, claystone, and mudstone),

Fig. 2. Little River q_t/q_u analysis using all boring locations with outliers removed. σ, standard deviation; CV, coefficient of variation. [Color online.]
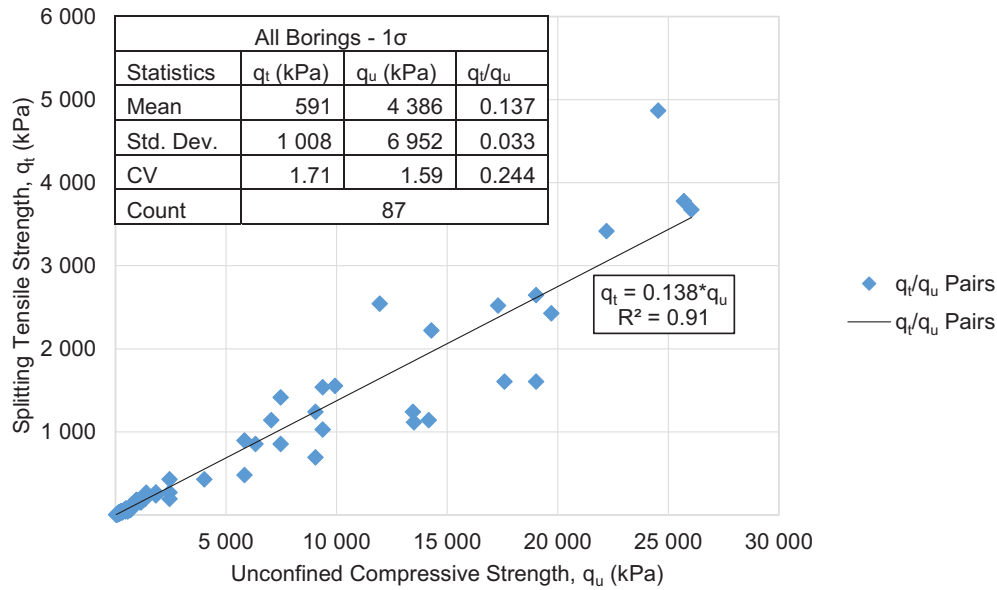

Table 2. Preliminary skin friction analysis at Little River.

Section	Skin friction, f_s (kPa)		Error (%)
	Load test	Monitoring	
SG7 to SG6	1010	996	−1.42
SG6 to O-cell	986	1096	11.17
O-cell to SG5	1025	977	−4.67
SG5 to SG4	651	666	2.21
Average	919	934	1.82

(6) $$M = 2.065 + 0.231(\log q_u)^2$$

and arenaceous materials with strong crystals and poorly developed crystal cleavage (e.g., sandstone and calcarenite),

(7) $$M = 2.065 + 0.270(\log q_u)^2$$

With the understanding that Florida field drilling would likely pass through varying layers of each material group, all three M equations were considered for the development of the Florida geomaterials q_t/q_u vs. q_u relationship. Using Johnston's equations for M and B, the following regression curves and equations (Fig. 3) were developed for each material group using q_u values ranging from approximately 7 to 70 000 kPa (1 to 10 000 psi).

Evident in Fig. 3, the shape and q_t/q_u ratios of the three regression curves are different with respect to q_u. Of interest was developing a single equation that was representative of all three curves to provide a good approximation of tensile strength (and therefore skin friction) in real time, regardless of the Florida geomaterial type encountered. The approach seemed justified as Johnston's limestone equation, used with McVay et al., produced overestimates of skin friction at Little River, where small varying layers of OC clay, IGM, and limestone were encountered. The overestimates were thought to be a result of Johnston's limestone datasets not including any samples from Florida to develop the equation. The limestone and dolomite datasets Johnston used to develop the equation had a compressive strength range of approximately 37 000 to 517 000 kPa. This would be considered very high strength limestone in Florida, even for the low end of the range

(37 000 kPa). The frequency distribution presented in Fig. 4, which includes q_u data collected from 23 different sites throughout Florida, indicates that over 90% of Florida limestone has a compressive strength less than 35 000 kPa. This led to the conclusion that Johnston's limestone datasets (carbonate materials) lacked the necessary low strength data needed to properly develop the relationship over the full compressive strength range. However, Johnston stated that despite the apparent radical differences between lightly OC clays, extremely hard rocks, and all the materials in between, their intact strength variations may be a matter of degree rather than of a fundamental nature. The statement suggests that a single equation could be developed to describe the mechanical behavior of all three sedimentary rock groups. Interestingly, Johnston's OC clay and IGM datasets (argillaceous materials) included siltstone, claystone, mudstone, marl, and OC clay, which are commonly found in central and north Florida, while his sandstone datasets (arenaceous materials) included sandstone and calcarenite (e.g., oolite and sandy limestone), which are found in south Florida and coastal areas. Moreover, taking all three datasets into consideration extends the compressive strength range from 10 to 517 000 kPa. Consequently, a new M equation was developed that is representative of all three material groups.
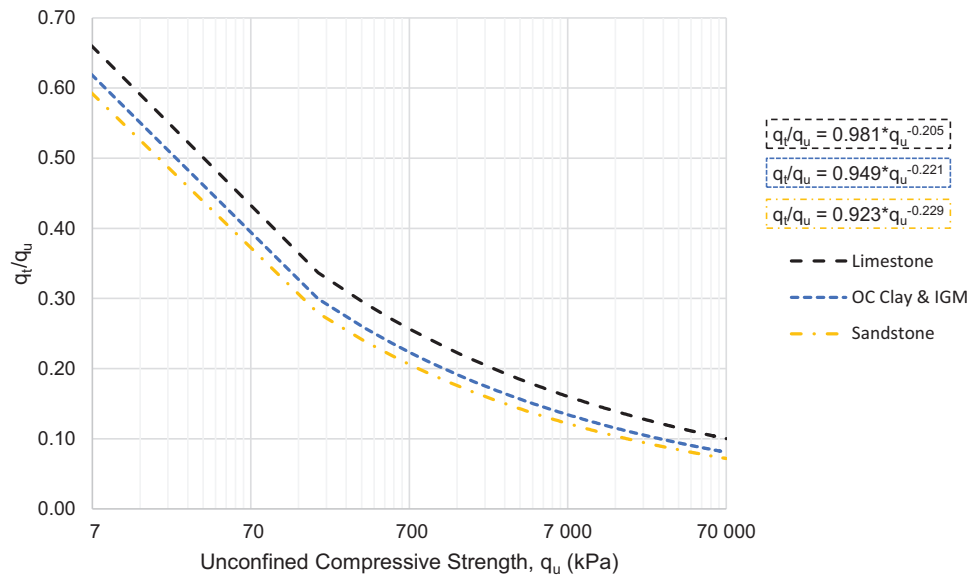
Equation development was completed using only data (core, load test, and MWD) collected at the Little River Bridge site, where varying layers of OC clay, IGM, and limestone were encountered, which is representative of two of Johnston's sedimentary M equations. Additionally, recovered cores from the site indicated a compressive strength range of approximately 30–30 000 kPa, which accounts for nearly 90% of Florida limestone compressive strengths (Fig. 4). Johnston's limestone M equation was adjusted to align the side shear prediction (MWD) with the load test data and a best fit equation was derived for simplified calculation, similar to Fig. 3. The adjustment began by plotting data points (q_t/q_u vs. q_u) in the q_u axis based on measured q_u values from the cores extracted at the Little River site. This placed emphasis in various portions of the q_u range that are commonly encountered in Florida's highly variable geological formations. As a result, the log multiplier in Johnston's limestone M equation was reduced from 0.170 to 0.158, and the curve was reshaped to reflect natural Florida conditions. Reduction factors were then applied to the newly derived best fit equation until the predicted side shear aligned with the load test results, which produced the following equation:

Table 3. Core data from Little River that indicates samples 4 and 5 are dissimilar materials.

Sample No.	Test type	Moisture (%)	Dry unit weight (kN/m³)	Max. load (kN)	q_t (kPa)	q_u (kPa)
1	T	59.8	9.9	0.2	44.8	—
2	U	58.2	10.2	0.6	—	262.7
3	T	60.1	9.9	0.3	55.8	—
4	U	69.0	9.4	0.3	—	116.5
5	T	3.2	24.5	42.3	6723.8	—
6	T	3.8	21.2	14.1	2256.7	—
7	U	5.1	21.1	23.7	—	7700.8
8	T	7.6	20.7	9.2	1503.7	—
9	T	4.8	23.5	4.6	739.8	—
10	T	61.3	9.9	0.2	27.6	—
11	T	28.8	14.4	0.2	35.9	—

Note: T, split tension (q_t); U, unconfined compression (q_u).

Fig. 3. q_t/q_u vs. q_u relationship for various geomaterials using Johnston's criteria. [Color online.]

$$q_t/q_u = 0.981 * q_u^{-0.205}$$
$$q_t/q_u = 0.949 * q_u^{-0.221}$$
$$q_t/q_u = 0.923 * q_u^{-0.229}$$

Limestone
OC Clay & IGM
Sandstone

$$(8) \qquad M = 3.304 + 0.158(\log q_u)^2$$

where q_u is measured in kilopascals (kPa).

As seen in eq. (8), aligning the side shear prediction increased Johnston's asymptotic M value of 2.065 to 3.304. Johnston stated in his report that it was quite feasible that the asymptotic value could range from 1.8 to 3.7, and the adjustment seems reasonable. Interestingly, the increased value reduces the q_t/q_u ratio as q_u approaches 0 and provides a similar q_t/q_u relationship to Johnston's sandstone equation at lower compressive strengths, even though arenaceous materials were not encountered at the site. The resulting curve now transitions through the sandstone and OC clay and IGM curves at lower compressive strengths, and provides a similar q_t/q_u relationship to Johnston's limestone equation at higher compressive strengths. This can be seen in Fig. 5, where the new Florida geomaterials M equation (eq. (8)) is compared with the original equations from all three material groups.

Evident in Fig. 5, the q_t/q_u ratios for the lower end q_u values are more representative of the sandstone curve and as q_u increases the q_t/q_u ratios become representative of the OC clay and IGM curve. As q_u progresses further, the Florida geomaterials curve gradually becomes more representative of Johnston's original limestone curve. Therefore, the side shear alignment approach, using only data collected at Little River, produced a new M equation that is representative of all three of Johnston's sedimentary relationships. It should be noted that the developed M equation is not intended to define a specific sedimentary material group within a specified portion of the q_u range; rather, it is to provide a general q_t/q_u relationship for Florida sedimentary rocks within a q_u range typical of Florida conditions. The purely theoretical relationship was further investigated on this basis.

Investigation of the new Florida geomaterials q_t/q_u correlations

From the FDOT bridge foundation database, extensive core data were available to investigate the q_t/q_u relationship of Florida geomaterials (as partially summarized in Fig. 4). Of particular interest was the q_t/q_u relationship from the database compared with the Florida geomaterials relationship when similar moisture contents and dry unit weights are considered. Based on the logic of Table 3, it stands to reason both material properties can be used to identify similar geomaterials, which should allow the q_t/q_u relationship to be properly investigated. For instance, the dry unit weight indicates that similar materials make up a rock mass (i.e., similar mineralogy; Perras and Diederichs 2014) and when combined with moisture content the properties become representative of the void ratio and porosity of the material, which should be indicative of the void structure. This is confirmed by the $Gw\% = Se_{void}$ condition for geomaterials, where G is specific gravity, $w\%$ is moisture content, S is degree of saturation, and e_{void} is void ratio (Lambe and Whitman 1969). Furthermore, it has been well documented that an increase in moisture content or porosity reduces mechan-

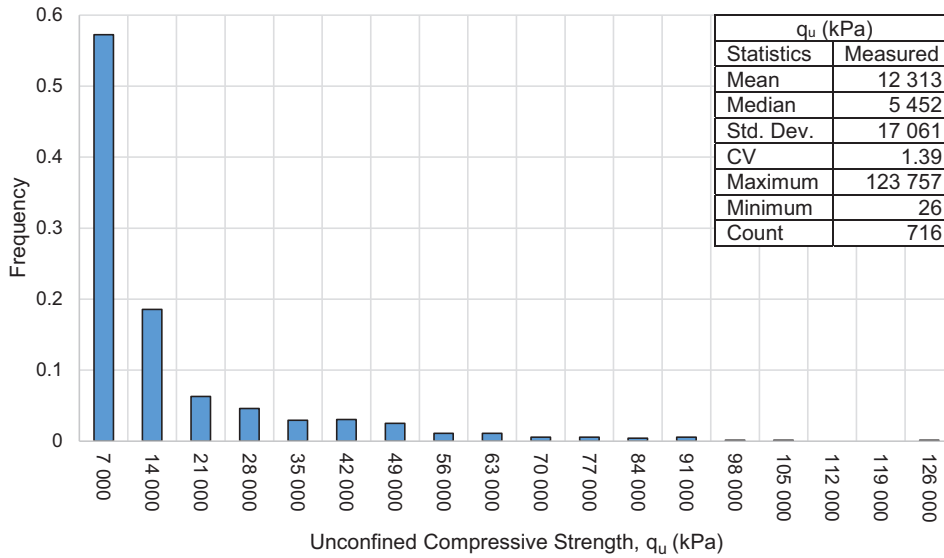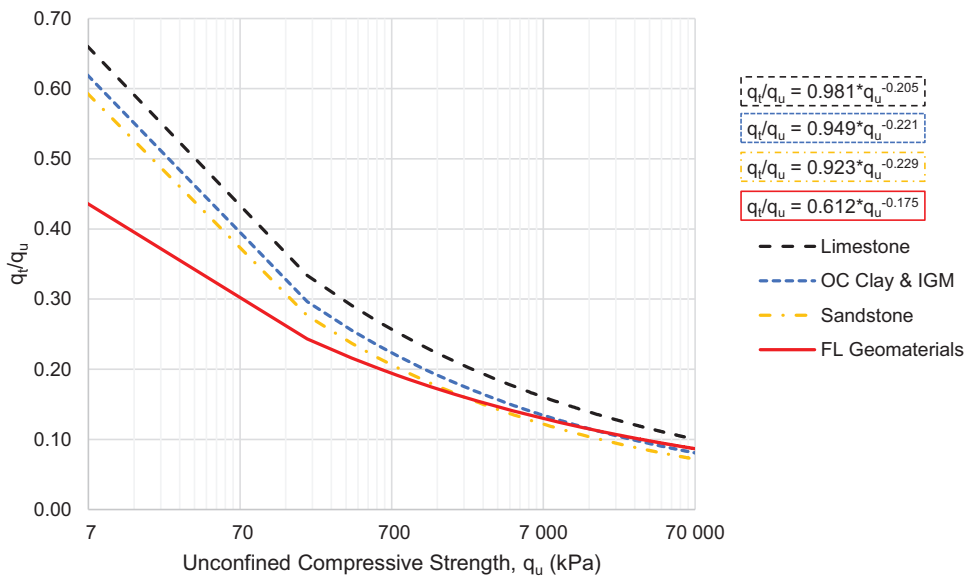**Fig. 4.** Frequency distribution of Florida limestone compressive strengths. [Color online.]

Fig. 5. Comparison of q_t/q_u vs. q_u curves with the new Florida geomaterials curve. [Color online.]

ical strength properties (Baud et al. 2014; Chen et al. 2013; Rajabzadeh et al. 2012; Vasarhelyi and Van 2006; Wong et al. 2016; Yilmaz 2010). Therefore, correlations between material properties and mechanical properties were investigated using approximately 1200 laboratory-tested q_t values and 700 laboratory-tested q_u values from the following project sites in Florida:

- 17th Street Causeway
- Acosta Bridge
- BR720153 SR-9 (I-95) Overland
- CR-326 at Waccasa River
- HEFT/SR 874 PD&E
- I-295 Buckman Bridge
- I-295 Dames Point Bridge
- I-95 at I-295 Cloverleaf
- I-95 Fuller Warren Bridge
- Jewfish Creek
- MIC- People Mover Project
- NW 12th Ave (SR 933) Miami River Bridge
- NW 36th Street Bridge

- Pump Station at Bal Harbour (96th St. and Indian Creek)
- Radio Tower Everglades Academy (Florida City)
- SR-10 atCSX RR (Beaver St. Viaduct), Duval Co.
- SR-20 at Lochloosa Creek, Alachua Co.
- SR-25 at Santa Fe River
- SR30/US98 at Aucilla River
- SR-9 (I-95) Overland Bridge
- US-90 Victory Bridge
- Verona Ave Bridge over Grand Canal
- Wall at Service Road South of Snake Creek

For the investigation, the individual q_u and q_t values from the dataset were grouped in ranges based on their material properties, moisture content (w%), and dry unit weight (γ_d). For moisture content, the ranges were grouped in increments of 2% (e.g., w% = 0%–2%, 2%–4%, etc.). For dry unit weight, the ranges were grouped in increments of approximately 0.8 kN/m³ (e.g., γ_d = 14.9–15.7 kN/m³, 15.7–16.5 kN/m³, etc.). For each material property range, the average and standard deviation were derived and used to establish an acceptable strength range for both q_u and q_t, which is used as an

Fig. 6. Core data index plot, unconfined compressive strength vs. moisture content. [Color online.]

$$q_u = 36\ 432 * (w\%)^{-0.817}$$
$$R^2 = 0.90$$
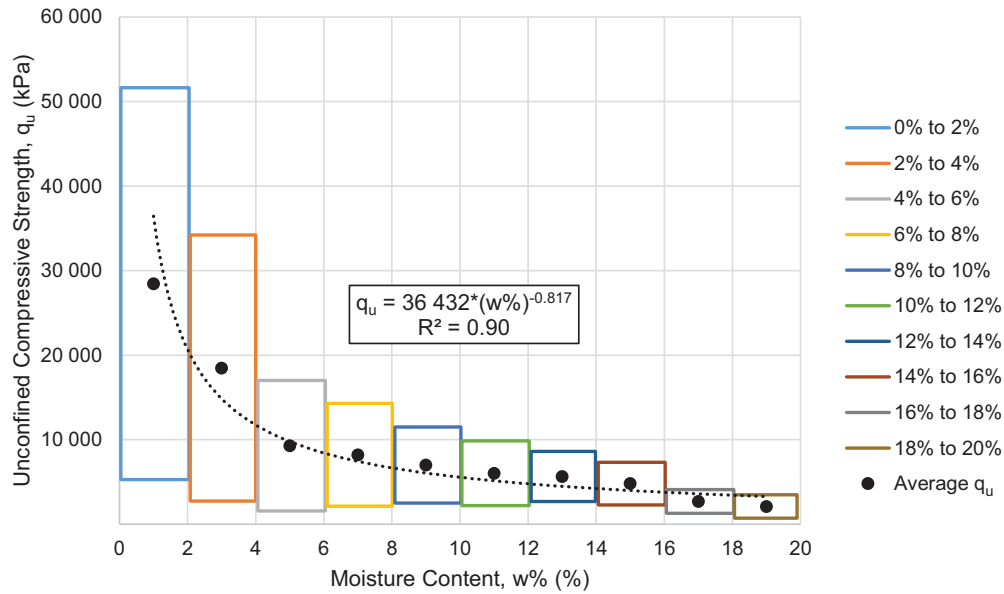
Fig. 7. Core data index plot, splitting tensile strength vs. moisture content. [Color online.]

$$q_t = 5\ 984 * (w\%)^{-0.775}$$
$$R^2 = 0.67$$
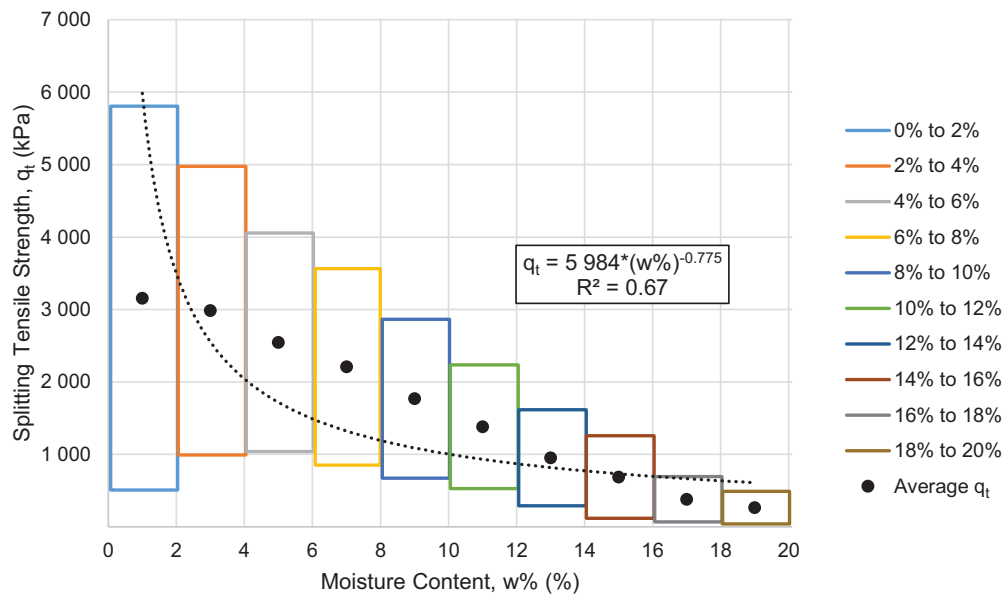
index reference for strength. The mechanical properties were then plotted as a function of each material property, and regression equations were developed using a best-fit power function derived from the averages of each material property range, Figs. 6 through 9. The average values were used to remove the influence of a specific material property range with more collected data affecting the overall relationship, thus allowing the typical strengths obtained within each material property range to be compared directly without bias.

As seen in all four "core data index" (CDI) plots, both material properties do influence both mechanical properties. The R^2 values derived in each CDI plot indicate that dry unit weight provides better correlation with q_u and q_t than does moisture content. Also observed in all cases except Fig. 7, the regression curves plotted within one standard deviation from the mean of each material property range. The averages within each material property range in Fig. 7 could have been more accurately defined through a linear or higher order polynomial curve fit. However, the intent was not

to produce an equation to perfectly fit the averages, as they can be compared directly without curve fitting; it was to investigate how each material property relates to the q_t/q_u relationship that is best defined by a power function as observed in Figs. 3 and 5.

Using the regression equations from Figs. 6–9, a best fit q_u and q_t value was generated from each material property range and paired with the respective strength value. For example, q_u was paired with q_t from the moisture content range 0%–2%, and q_u was paired with q_t from the dry unit weight range 14.9–15.7 kN/m³. This was also done using the average values from each material property range. The split tension values were then converted to direct tension using Perras and Diederichs' (2014) recommendations for sedimentary rocks (direct tension = 0.70(split tension)). Using the best fit and average CDI values, q_t was plotted vs. q_u and compared with the Florida geomaterials equation separately.

As observed in Figs. 10 and 11, using either the best fit or average values from the CDI plots (Figs. 6–9) produced nearly identical equations to the curve-fitted Florida geomaterials equation. Thus,

Fig. 8. Core data index plot, dry unit weight vs. unconfined compressive strength. [Color online.]
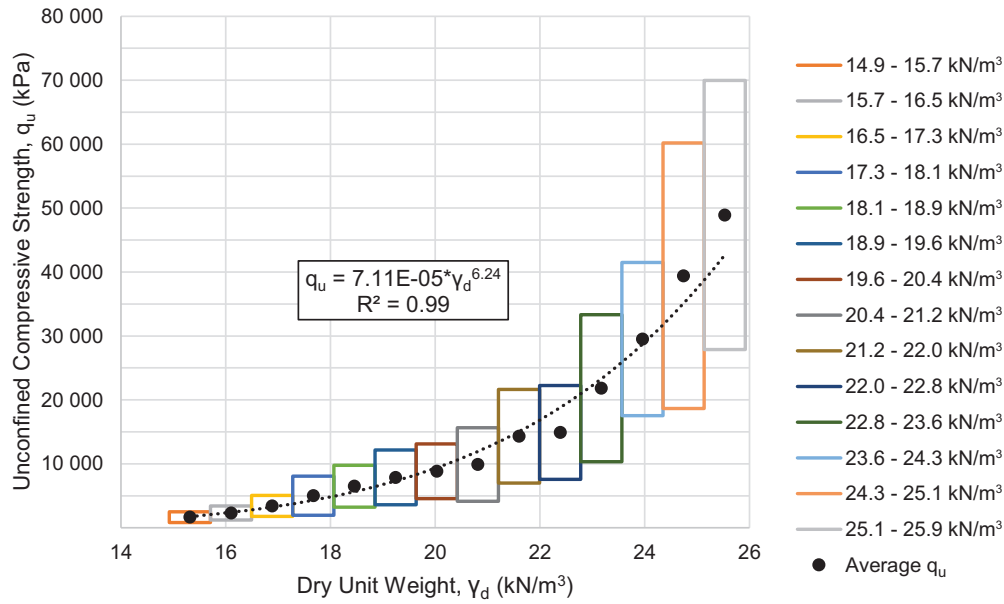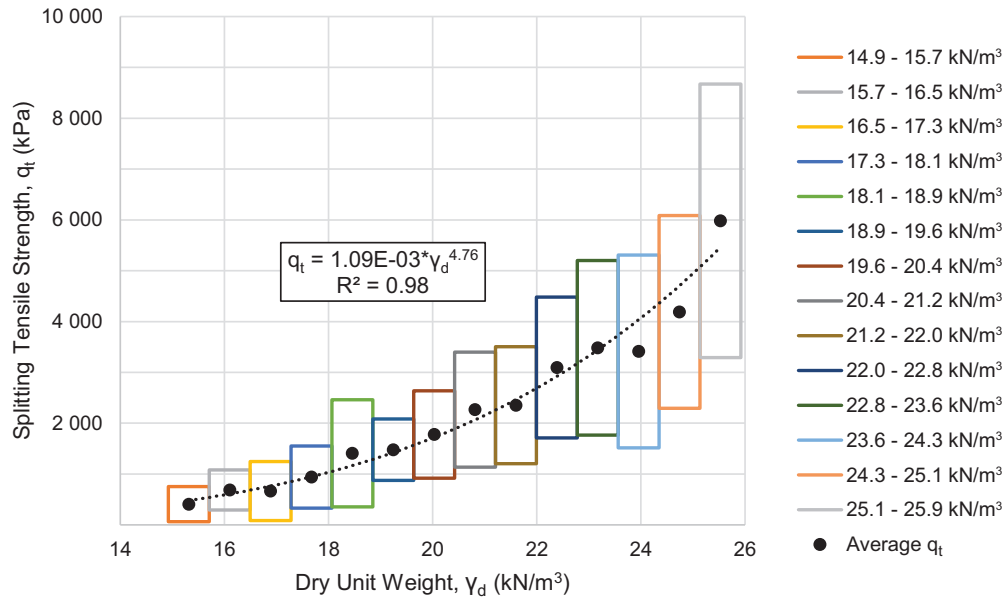

Fig. 9. Core data index plot, dry unit weight vs. splitting tensile strength.

the same q_t/q_u relationship was found using a theoretical approach and an empirical approach. All three relationships were further investigated to determine which should be used during final side shear assessment with McVay et al.

Using the available split tension data from the FDOT database, predictions of q_u were made using the developed relationships: Florida geomaterials (FL Geo.), CDI average (CDI - Avg.), and CDI best fit (CDI B.F.). The CDI predictions were made without Perras and Diederichs' (2014) reduction applied, and the Florida geomaterials predictions were made with the reduction applied to convert direct tension to split tension (split tension = (direct tension)/ 0.70). The predicted q_u values were then compared with the measured values presented in Fig. 3. The frequency and cumulative frequency distributions used in the comparison are provided in Figs. 12 and 13.

In all cases, the predicted values compared favorably with the measured values. The Florida geomaterials and CDI best fit pre-

dictions were nearly identical and both provided better prediction than the CDI average predictions. The Florida geomaterials equation was determined to be the most accurate based on average compressive strength, the coefficient of variability, and the trends of the measured and predicted data over the full compressive strength range. This is more apparent in the cumulative frequency distribution (Fig. 13). Therefore, the Florida geomaterials equation was used during final side shear assessment. From Figs. 10 and 11, expressing the Florida geomaterials equation as q_t vs. q_u for skin friction assessment gives

$$(9) \qquad q_t = 0.612 q_u^{0.825} \text{ (kPa)}$$

Comparative skin friction analysis

Drilled shaft MWD provides a means to measure unconfined compressive strength in real time during the shaft installation

Fig. 10. Comparison of CDI best fit values q_t vs. q_u relationship with the Florida (FL) geomaterials equation. [Color online.]
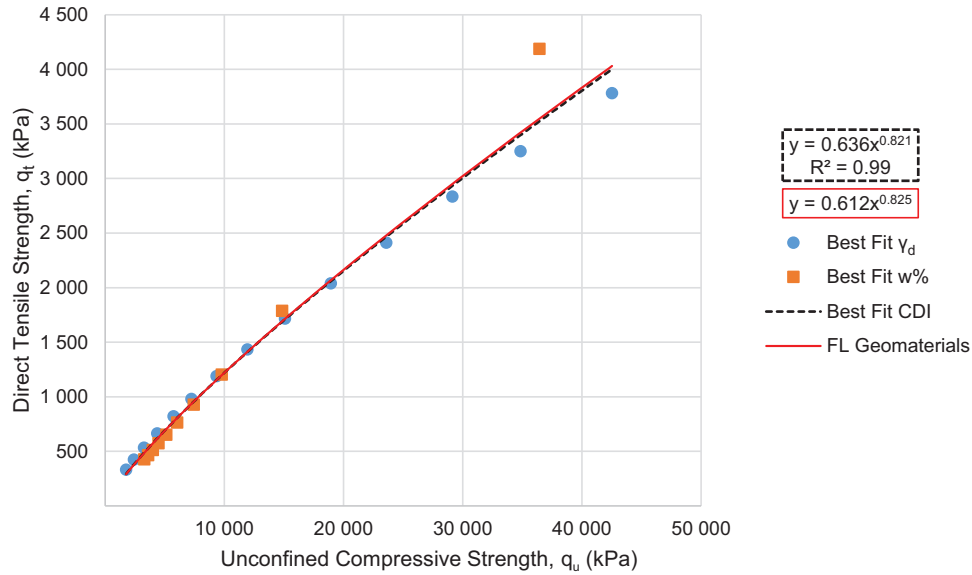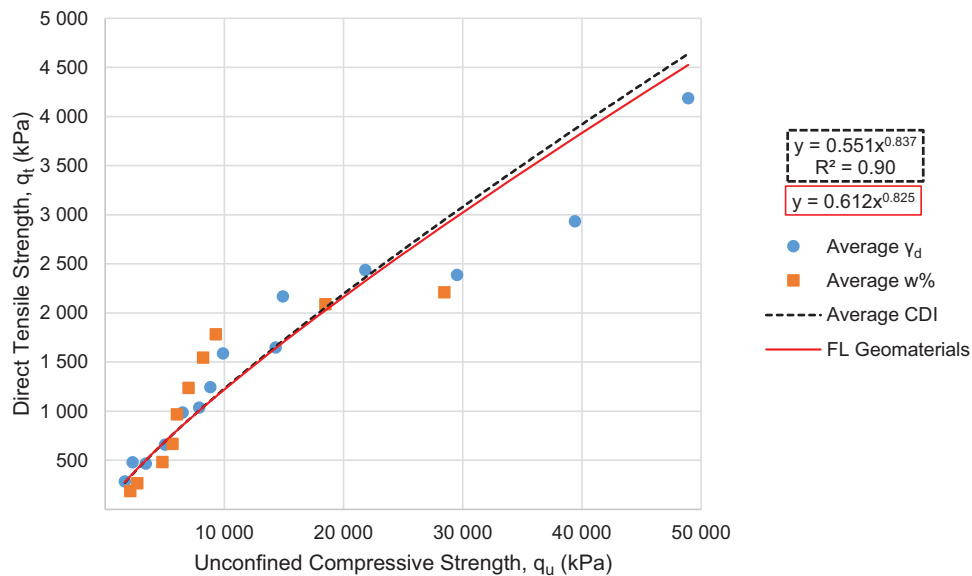

Fig. 11. Comparison of CDI average values q_t vs. q_u relationship with the Florida geomaterials equation. [Color online.]

process. In addition, the developed q_t/q_u relationship presented allows the foundation engineer to choose from any of the leading skin friction equations (Table 1), which are generally used in Florida drilled shaft design based on measures of compressive strength. A comparative skin friction analysis was conducted using each method at all three monitored shaft locations (Tables 4 and 5). The shaft segments included in the analysis were all fully mobilized during load testing and provided direct comparison with the predicted results from MWD.

Evident from Tables 4 and 5, several methods provided reasonable skin friction estimates compared to the load test results. Reese and O'Neill's (1987) recommended equation, developed by Horvath and Kenney (1979), provided a good conservative estimate at all three locations. Gupton and Logan's (1984) equation provided an excellent result at Kanapaha and Overland, and reasonable overestimates at Little River. This was expected as the equation was only intended for use in weaker rock found in south Florida and not higher strength limestone found in the panhandle (e.g., Little River). The McVay et al. method, which was developed

for weak, moderate, and high strength Florida limestone, used in conjunction with the Florida geomaterials equation produced the best results. The method was in excellent agreement with the load test results at all three monitored locations and the average error was negligible. Furthermore, the method produced nearly identical results to Gupton and Logan's equation in weaker rock. This suggests that the McVay et al. method, used with the Florida geomaterials equation, should also be accurate in south Florida limestone formations (arenaceous geomaterial), where monitoring did not occur during this research. Consequently, McVay et al. was chosen as the recommended equation to use with the developed drilled shaft MWD method in Florida limestone.

For convenience, the Florida geomaterials equation was incorporated into the equation developed by McVay et al. so skin friction could be estimated directly from q_u. The following provides the equation development:

Substituting the Florida geomaterials equation (eq. (9)) into the skin friction equation developed by McVay et al.,

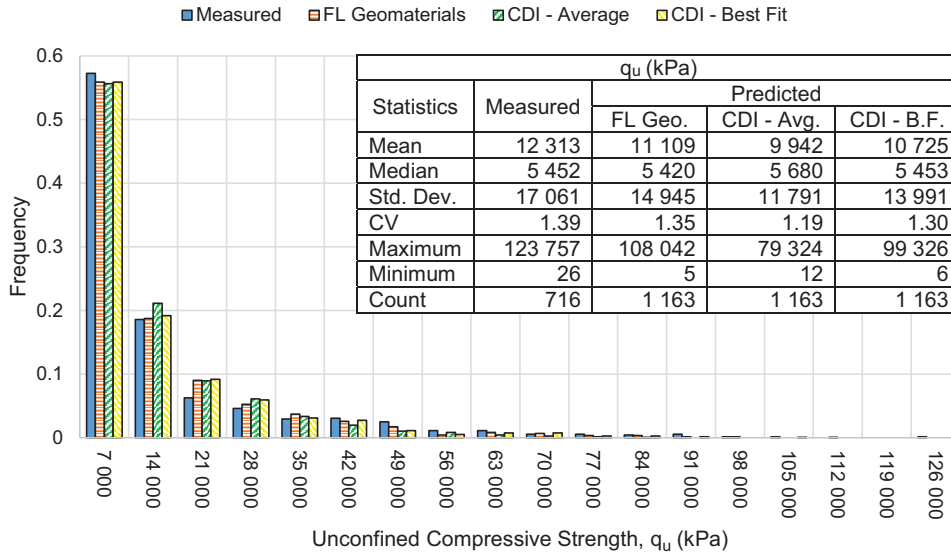**Fig. 12.** Frequency distribution comparing predicted q_u values with measured q_u values. [Color online.]

Statistics	Measured	q_u (kPa) Predicted		
		FL Geo.	CDI - Avg.	CDI - B.F.
Mean	12 313	11 109	9 942	10 725
Median	5 452	5 420	5 680	5 453
Std. Dev.	17 061	14 945	11 791	13 991
CV	1.39	1.35	1.19	1.30
Maximum	123 757	108 042	79 324	99 326
Minimum	26	5	12	6
Count	716	1 163	1 163	1 163

Fig. 13. Cumulative frequency distribution comparing predicted q_u values with measured q_u values. [Color online.]
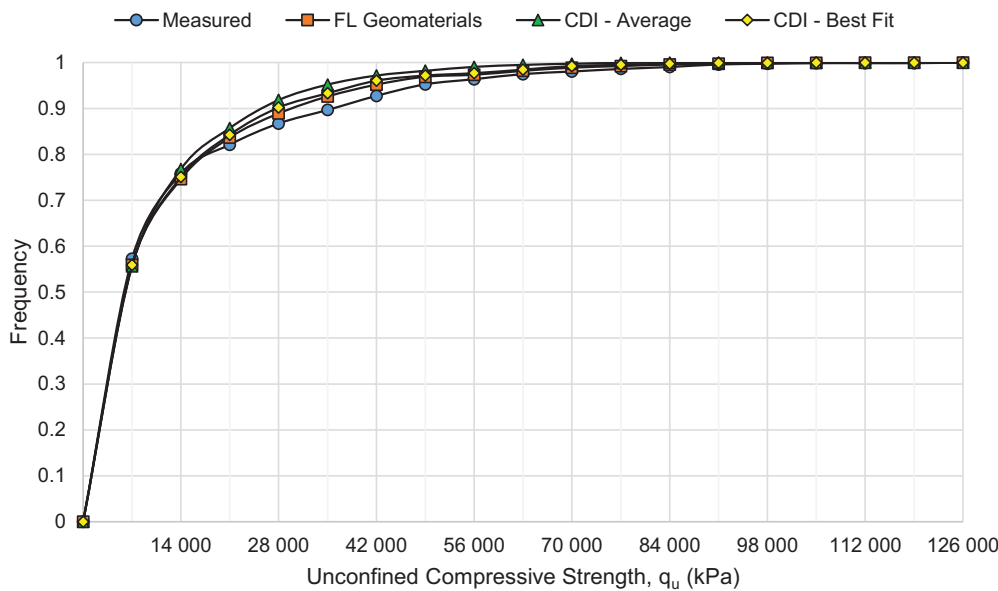
(10) $\quad f_s = \dfrac{1}{2} q_u^{0.5} q_t^{0.5}$

f_s can be solved directly using only q_u

(11) $\quad f_s = 0.3912 q_u^{0.9125}$

With the final drilling equation developed to measure skin friction directly during shaft installations, additional analysis was performed to provide a better understanding of the monitoring accuracy and the variability of the results. Table 6 presents the monitoring results vs. the load test results for skin friction at each monitored location using the new equation. Again, the presented results are in portions of the shafts at each location where the skin friction was fully mobilized; thereby providing direct comparison of MWD to conventional methods for estimating shaft capacity. A different load test method was used at each of the sites, providing comparison with the three most conventional load test methods.

As seen in Table 6, the percent difference between the MWD and load test results revealed a relatively small range of variability, which was confirmed by conducting a bias analysis (i.e., the ratio of measured/predicted values). From the analysis, the mean and median bias were both found to be 1.00 and the coefficient of variation (CV) was less than 0.07 (Table 7 and Fig. 14). The results indicate that drilled shaft construction monitoring, via MWD, is a viable solution to reducing spatial uncertainties and providing accurate measurements of compressive strength and skin friction in real time.

Conclusions and recommendations

Conclusions
The following conclusions were drawn from this study:

- The developed monitoring method is a viable option for estimating rock strength and drilled shaft capacity in real time. This is based on compressive strength comparisons with core data obtained from traditional rock coring (Rodgers et al. 2018b)

Table 4. Skin friction comparative analysis using unit side shear methods 1 through 5.

Location	Section	f_s (kPa) Load test	(1)	(2)	(3)	(4)	(5)
Little River	SG8 to SG7	474	534	425	312	550	849
	SG7 to SG6	1010	942	805	411	670	1609
	SG6 to O-cell	986	1058	891	469	748	1781
	O-cell to SG5	1025	932	789	421	687	1578
	SG5 to SG4	651	668	537	365	623	1074
Kanapaha	TS SG1 to SG2	384	413	313	288	526	626
	TS SG2 to SG3	394	392	295	279	515	591
	TS SG4 to Base	233	234	169	210	417	337
	ES SG1 to SG2	113	113	78	123	261	156
Overland	Segment 2	99	91	60	123	280	120
Average percent error		N/A	0.6%	−22.2%	−27.9%	38.3%	55.6%

Table 5. Skin friction comparative analysis using unit side shear methods 6 through 10.

Location	Section	f_s (kPa) Load test	(6)	(7)	(8)	(9)	(10)
Little River	SG8 to SG7	474	566	293	501	674	693
	SG7 to SG6	1010	1073	386	781	889	1190
	SG6 to O-cell	986	1187	441	733	1015	1358
	O-cell to SG5	1025	1052	396	730	910	1218
	SG5 to SG4	651	716	343	606	790	1057
Kanapaha	TS SG1 to SG2	384	417	271	414	623	833
	TS SG2 to SG3	394	394	263	389	604	809
	TS SG4 to Base	233	225	197	426	454	607
	ES SG1 to SG2	113	104	116	226	266	356
Overland	Segment 2	99	80	116	200	266	356
Average percent error		N/A	3.7%	−32.2%	21.4%	56.0%	104.2%

Table 6. Skin friction comparative analysis summary using eq. (11).

Location	Reference	Section	Test type	Thickness (m)	Skin friction Measured (kPa)	Skin friction Predicted (kPa)	% difference
Little River	LR-1	SG8 to SG7	Osterberg	3.05	474	534	12.63
	LR-2	SG7 to SG6	Osterberg	1.52	1 010	942	−6.78
	LR-3	SG6 to O-cell	Osterberg	1.68	986	1 058	7.23
	LR-4	O-cell to SG5	Osterberg	1.07	1 025	932	−9.07
	LR-5	SG5 to SG4	Osterberg	1.52	651	668	2.57
Kanapaha	K-1	SG1 to SG2	Static	0.91	384	413	7.48
	K-2	SG2 to SG3	Static	0.91	394	392	−0.49
	K-3	SG4 to Base	Static	0.61	233	234	0.41
	K-4	East Shaft	Static	1.52	113	113	0.00
Overland	O-1	Segment 2	Statnamic	1.52	99	91	−7.77
Average	N/A	All	All	1.43	537	538	0.62

Table 7. Unit side shear bias analysis summary of statistics.

| Statistics	Bias
Average	1.00
Median	1.00
Std. Dev.	0.068
CV	0.068
Count	10

and skin friction estimations compared to three of the most widely used load testing methods (i.e., Osterberg, Statnamic, and top-down (traditional) static load testing).

- Equipment needed to monitor drilled shaft installations is often standard on new drill rigs and is commercially available for rig types without monitoring equipment (Rodgers et al. 2018b).

This provides an easy transition to incorporate the developed method into standard drilled shaft practice.

- The developed method provides a means to quantify the quality and length of rock sockets in real time during the drilling process. This ensures the as-built foundation meets or exceeds the engineering design in real time and provides a new method of quality control for both the drilling contractor and foundation engineer.
- This research took the first steps towards reducing spatial variability concerns for structures supported by drilled shafts. Monitored drilling practices (MWD) should ultimately lead to increased resistance factors used in design. This will provide more efficient and cost-effective construction practices by reducing the time of completion and cost per shaft based on reduced uncertainty (AASHTO 2009).
- It was found that there is an interdependence between the compressive and tensile strengths of Florida geomaterials. In

Fig. 14. Unit side shear bias analysis measured/predicted (load test / monitoring). [Color online.]
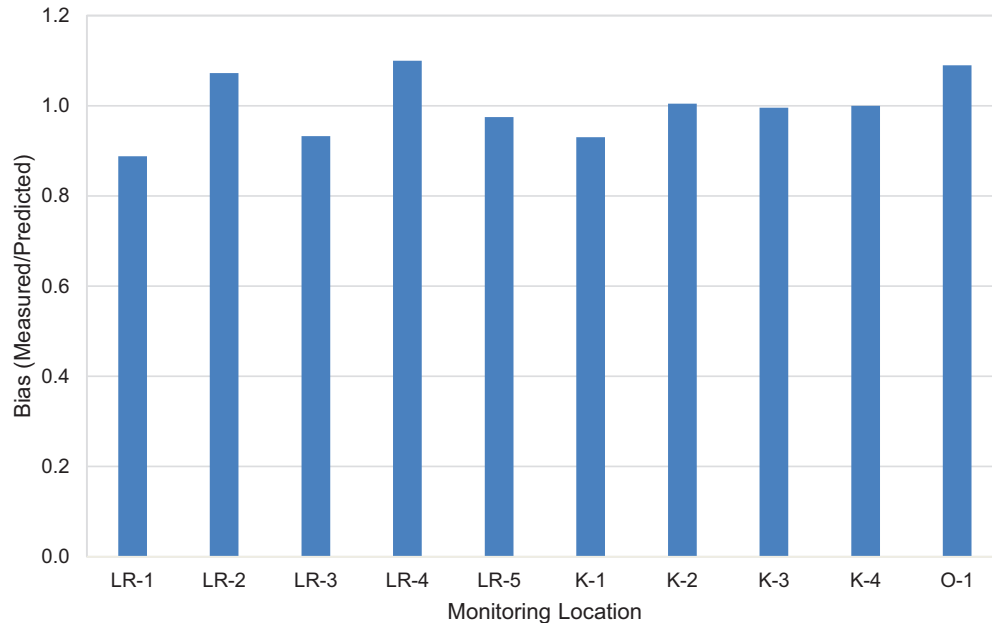
addition, new relationships were developed between material and mechanical properties. Correlations were discovered between mechanical properties (compressive and tensile strength) and material properties (dry unit weight and moisture content). This gives rise to the concept of index testing, where mechanical properties could be estimated from material properties that are easy to obtain. Core data index testing would provide a better understanding of geomaterial mechanical properties when core data are limited for sites with poor recoveries.

Recommendations

The following recommendations are based on the findings from this study:

- Conduct more drilled shaft monitoring with load tests to further validate the developed approach.
- The concept of MWD should be adapted to more geotechnical engineering applications.
- MWD should be developed for auger cast-in-place (ACIP) piles where visual inspection of the drilled cuttings does not occur. This would provide reliability for a deep foundation type that is steadily gaining popularity for its ease of construction and efficiency.
- MWD should also be used as a site investigation tool on standard penetration test (SPT) rigs to provide additional data used for geotechnical engineering design purposes. This would provide continuous measurements of rock strength and a means to quantify the quality of the coring procedure. Incorporating the developed method onto a SPT rig would provide continuous measurements, similar to a cone penetration test (CPT), with the ability to penetrate through layers of rock, which terminates a CPT. The method should be used while advancing the hole with a roller bit and during coring with a core barrel.
- The concept of index testing should be explored for dry unit weight, moisture content, porosity, and carbonate content. This will provide an estimated reference of strength for sites with poor recoveries.
- Finally, this research specifically focused on reducing the uncertainty of drilled shafts socketed into Florida limestone, as a very high degree of variability is typically encountered throughout the state. However, the concept of monitoring drilled shaft

installations could easily be translated to any rock type when coupled with a load testing program. This is achieved through measurements of specific energy recorded during the excavation of load-tested shafts. As measurements of specific energy (Teale 1965) only rely on drilling parameters torque, crowd, rotational speed, penetration rate, and bit diameter, and not the Florida-specific correlations developed in this research, an acceptable limit of required specific energy could be established based on the results of the load test. This would provide a minimum requirement of specific energy that must be achieved for each production shaft when drilling into layers of rock, IGM or OC clay. As a result, the insight gained from load testing would be translated directly to the production shafts and ensure the as-built foundations meet or exceed the expectations of the engineering design. This would alleviate concerns due to uncertainty and ultimately lead to the use of higher LRFD resistance factors, which reduces the overall construction costs associated with drilled shafts.

Wasman, Mike Faraone, Khiem Tran, Cary Peterson, and Anand Patil. Without their assistance, this research would not have been possible.

References

AASHTO. 2009. LRFD bridge design specifications. 4th ed. (2009 interim revisions.) American Association of State Highway and Transportation Officials, Washington, D.C.

Anoglu, N., Girgin, Z., and Anoglu, E. 2006. Evaluation of ratio between splitting tensile strength and compressive strength for concrete up to 120 MPa and its application in strength criterion. ACI Materials Journal, **103**: 18–24.

Baud, P., Wong, T., and Zhu, W. 2014. Effects of porosity and crack density on the compressive strength of rocks. International Journal of Rock Mechanics and Mining Sciences, **67**: 202–211. doi:10.1016/j.ijrmms.2013.08.031.

Brown, D., Turner, J., and Castelli, R. 2010. Drilled shafts: construction procedures and LRFD design methods. Publication No. FHWA-NHI-10-016, Federal Highway Administration, Washington, D.C.

Carter, J., and Kulhawy, F. 1987. Analysis and design of foundations socketed into rock. Research Report 1493-4, Geotechnical Engineering Group. Cornell University, Ithaca, New York.

Chen, X., Wu, S., and Zhou, J. 2013. Influence of porosity on compressive and tensile strength of mortar cement. Construction and Building Materials, **40**: 869–874. doi:10.1016/j.conbuildmat.2012.11.072.

Chung, J., Ko, J., Klammler, H., McVay, M., and Lai, P. 2012. A numerical and experimental study of bearing stiffness of drilled shafts socketed into heterogeneous rock. Computers & Structures, **90–91**: 145–152. doi:10.1016/j.compstruc.2011.09.004.

Florida Department of Transportation (FDOT). 2015. Soils and foundation handbook. Florida Department of Transportation, State Materials Office. Gainesville; Fla.

Gupton, C., and Logan, T. 1984. Design guidelines for drilled shafts in weak rocks of south Florida. *In* Proceedings of the South Florida Annual ASCE Meeting, ASCE.

Horvath, R., and Kenney, T. 1979. Shaft resistance of rock-socketed drilled piers. *In* Symposium on Deep Foundations, ASCE National Convention, Atlanta, Ga., pp. 182–214.

Johnston, I. 1985. Strength of intact geomechanical materials. Journal of Geotechnical Engineering, **111**: 730–749. doi:10.1061/(ASCE)0733-9410(1985)111:6(730).

Lambe, T.W., and Whitman, R.V. 1969. Soil mechanics. John Wiley & Sons, New York.

McVay, M., Townsend, F., and Williams, R. 1992. Design of socketed drilled shafts in limestone. Journal of Geotechnical Engineering, **118**(10): 1626–1637. doi:10.1061/(ASCE)0733-9410(1992)118:10(1626).

Perras, M., and Diederichs, M. 2014. A review of the tensile strength of rock: concepts and testing. Geotechnical and Geological Engineering, **32**: 525. doi:10.1007/s10706-014-9732-0.

Rajabzadeh, M., Moosavinasab, Z., and Rakhshanderhroo, G. 2012. Effects of rock classes and porosity on the relation between uniaxial compressive strength and some rock properties for carbonate rocks. Rock Mechanics and Rock Engineering, **45**(1): 113–122. doi:10.1007/s00603-011-0169-y.

Ramos, H., Antorena, J., and McDaniel, G. 1994. Correlations between the Standard Penetration Testing (SPT) and the measured shear strength of Florida natural rock. *In* Proceedings from the FHWA International Conference on Design and Construction of Deep Foundations, Orlando, Fla., pp. 699–711.

Reese, L., and O'Neill, M. 1987. Drilled shafts: construction procedures and design methods. Design manual. US Department of Transportation, Federal Highway Administration, McLean, Va.

Reynolds, R., and Kaderabek, T. 1980. Miami limestone foundation design and construction. ASCE, New York.

Rodgers, M., McVay, M., Ferraro, C., Horhota, D., Tibbetts, C., and Crawford, S. 2018*a*. Measuring rock strength while drilling shafts socketed into Florida limestone. Journal of Geotechnical and Geoenvironmental Engineering, **144**(3). doi:10.1061/(ASCE)GT.1943-5606.0001847.

Rodgers, M., McVay, M., Horhota, D., and Hernando, J. 2018*b*. Assessment of rock strength from measuring while drilling shafts in Florida limestone. Canadian Geotechnical Journal, **55**(8): 1154–1167. doi:10.1139/cgj-2017-0321.

Rowe, R., and Armitage, H. 1987. A design method for drilled piers in soft rock. Canadian Geotechnical Journal, **24**(1): 126–142. doi:10.1139/t87-011.

Teale, R. 1965. The concept of specific energy in rock drilling. International Journal of Rock Mechanics and Mining Sciences & Geomechanics Abstracts, **2**: 57–73. doi:10.1016/0148-9062(65)90022-7.

Vasarhelyi, B., and Van, P. 2006. Influence of water content on the strength of rock. Engineering Geology, **84**(1–2): 70–74. doi:10.1016/j.enggeo.2005.11.011.

Williams, A., Johnston, I., and Donald, I. 1980. The design of socketed piles in weak rock. *In* Proceedings of the International Conference on Structural Foundations in Rock, the Netherlands, pp. 327–347.

Wong, L., Maruvanchery, V., and Liu, G. 2016. Water effects on rock strength and stiffness degradation. Acta Geotechnica, **11**(4): 713–737. doi:10.1007/s11440-015-0407-7.

Yilmaz, I. 2010. Influence of water content on the strength and deformability of gypsum. International Journal of Rock Mechanics and Mining Sciences, **47**(2): 342–347. doi:10.1016/j.ijrmms.2009.09.002.